Letter

Thermodynamic performance bounds for radiative heat engines

Maxime Giteau,* Michela F. Picardi, and Georgia T. Papadakis†
ICFO - The Institute of Photonics Sciences, Castelldefels, Barcelona, Spain

(Received 14 July 2023; revised 7 September 2023; accepted 11 December 2023; published 20 December 2023)

Heat engines cannot generally operate at maximum power and efficiency, imposing a trade-off between the two. Here, we highlight the exact nature of this trade-off for engines that exchange heat radiatively with a hot source. We derive simple analytical expressions for the performance bounds of reciprocal and nonreciprocal radiative heat engines. We also highlight that radiative engines can achieve a better power-efficiency trade-off than linear ones. These bounds are especially relevant for thermophotovoltaics, offering useful metrics against which to compare device performance.

DOI: 10.1103/PhysRevApplied.20.L061003

Heat engines are ubiquitous for energy applications, allowing power generation from any heat source. Heat engines that can deliver substantial power at high efficiency are earnestly sought after, as any marginal performance increase promises tremendous economic returns due to the large markets involved [1]. To optimize the operation of heat engines, it is crucial to understand their performance bounds, particularly the trade-off between power output and efficiency. Thermodynamics, which analyzes energy and entropy flows at the macroscopic level, offers an ideal framework to determine these bounds.

Radiative heat engines are a class of nonlinear engines that exchange heat as thermal radiation. One practical implementation of such engines is thermophotovoltaics (TPVs), where a photovoltaic cell directly converts the thermal radiation emitted by a hot source into electricity [2]. TPVs is a very active and promising research field, with many impressive results reported recently, both in terms of efficiency [3,4] and power output [5]. TPV devices are particularly appealing for energy conversion at very high temperatures (above 1000°C, a region where efficiencies well above 50% are theoretically possible) for applications such as thermal energy storage [6]. Therefore, establishing the general performance bounds of TPV devices is both worthwhile and timely.

The efficiency of any heat engine operating between a hot source at temperature T_H and a cold sink at temperature T_C is bounded by the Carnot limit $\eta_C = 1 - T_C/T_H$ [7]. However, except for very particular configurations [8–10], operating close to Carnot efficiency leads to vanishing power output. In that regard, it is well known that TPV systems can theoretically approach the Carnot efficiency in the limit of zero power output by considering a narrowband emitter [2].

At the same time, the power output bounds of radiative heat engines have been explored in great detail, particularly in the context of solar energy conversion, using both detailed balance models [11–13] as well as thermodynamic descriptions [14–18]. These bounds readily extend to radiative heat engines by adjusting the temperature of the hot and cold reservoirs. We emphasize that, as the power received from the sun is free (the sun is outside the conversion system), the term "efficiency" in the context of solar energy refers to normalized power density. Hence, the quantity being considered and optimized is the power output. Additionally, the efficiency bound at maximum power, known as the Curzon-Ahlborn limit $\eta_{CA} = 1 - \sqrt{T_C/T_H}$ for linear heat engines [19,20], has been generalized to nonlinear (and particularly radiative) heat engines in the context of endoreversible thermodynamics [21,22]. Finally, the efficiency and power output limits of single-, double-, and triple-junction TPV cells have been previously derived using a detailed balance formalism [23].

Despite these results, the general trade-off between power output and efficiency for radiative heat engines has not been previously investigated. Furthermore, while universal trade-off relations between power and efficiency have been identified [24,25], they do not provide specific answers for given classes of heat engines. As a result, the performance bounds of radiative heat engines (which encompass TPV systems) remain largely unidentified.

In this paper, we clarify the nature of the power-efficiency trade-off for radiative heat engines, determining the maximum power achievable by a radiative heat engine operating at any given efficiency. To do so, we generalize the thermodynamic formalism developed for solar energy-conversion limits, first introducing the well-known

*maxime.giteau.pro@gmail.com
†georgia.papadakis@icfo.eu

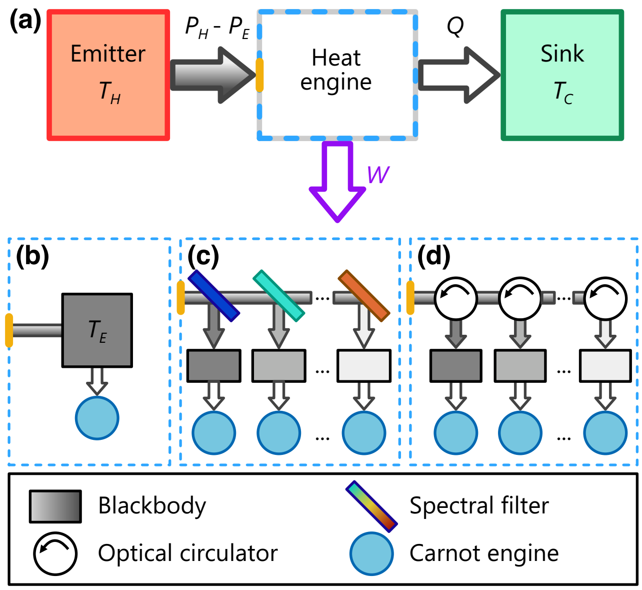

FIG. 1. (a) General representation of a radiative heat engine. (b)–(d) Different heat-engine models. (b) Endoreversible engine: a single blackbody coupled to a Carnot engine. (c) Infinite reciprocal engine. (d) Infinite nonreciprocal engine for isentropic conversion.

endoreversible engine model before deriving performance (i.e., power-versus-efficiency) bounds for reciprocal and nonreciprocal engines.

We consider a hot emitter at temperature T_H and a cold sink at temperature T_C, exchanging power in steady state through a heat engine. The emitter and the engine interact radiatively while the engine is in thermal contact with the sink. We call P_H and P_E the power densities emitted by the hot emitter and the engine, respectively. The radiative heat engine generates an output power density W with an accompanying heat flux Q. The system is schematically represented in Fig. 1(a). In the following, we do not account for near-field effects. We consider that the emitter and heat engine fully see each other (the emitter receives radiation from the heat engine from all directions, and vice versa). As a result, we only need to consider exchanged power *densities* (i.e., power per unit area). In TPVs, this means equating the system efficiency to the pairwise efficiency by assuming a lossless cavity [26].

We define a first figure of merit, ρ, as the output power density normalized to the power density emitted by a blackbody emitter at temperature T_H (note: this is how *efficiency* is defined for solar energy conversion):

$$\rho = \frac{W}{\sigma T_H^4}, \tag{1}$$

where σ is the Stefan-Boltzmann constant. In the following, we refer to this quantity as the power output. Meanwhile, the second figure of merit is the efficiency η, in which the denominator accounts for the net heat drawn from the emitter (the photons re-emitted towards the emitter do not count as a loss):

$$\eta = \frac{W}{P_H - P_E}. \tag{2}$$

With these definitions, $\rho \leq \eta$, since the net exchanged power must be smaller than the incoming blackbody radiation. In the following, we consider a blackbody emitter, such that $P_H = \sigma T_H^4$.

First, we present the performance limits of an endoreversible engine consisting of a single blackbody at temperature T_E coupled to a Carnot engine [Fig. 1(b)] [14,16]. Endoreversible means the converter itself is reversible (Carnot engine) while losses arise from the heat exchange with the hot and cold reservoirs. The power output and efficiency take the expressions:

$$\rho_E = \left[1 - \left(\frac{T_E}{T_H}\right)^4\right]\left[1 - \frac{T_C}{T_E}\right], \tag{3}$$

$$\eta_E = 1 - \frac{T_C}{T_E}. \tag{4}$$

From Eqs. (3) and (4), we obtain the *endoreversible model* (power-versus-efficiency) by sweeping the engine temperature T_E from T_C to T_H. Carnot efficiency is achieved in the limit $T_E \to T_H$, leading to zero power output. The maximum power output $\bar{\rho}_E$ is found by solving $4T_E^5 - 3T_C T_E^4 - T_C T_H^4 = 0$, leading to the so-called blackbody (or endoreversible) limit $\bar{\rho}_E = 85.36\%$ for solar energy conversion (when $T_H = 6000$ K and $T_C = 300$ K) [14–16]. We can also write a direct relation between ρ_E and η_E, independent of T_E:

$$\rho_E = \eta_E\left[1 - \left(\frac{T_C}{T_H}\right)^4 \frac{1}{(1-\eta_E)^4}\right]. \tag{5}$$

We emphasize that Eqs. (3) and (4) have been derived before, for example, in Ref. [16]. However, they do not impose performance bounds on radiative energy conversion. To derive general bounds, we consider two cases. In the first, the engine consists of an infinite number of endoreversible subengines, each converting an infinitesimal part of the incident radiation [Fig. 1(c)]. This case, detailed in the Supplemental Material [27], leads to the *reciprocal bound*, i.e., the upper bound for engines that obey time-reversal symmetry. However, as we will see, it only marginally surpasses the endoreversible model. The second case, presented below, allows for nonreciprocity, leading to the absolute performance bound for radiative energy conversion. We stress that, for both the reciprocal and nonreciprocal bounds, only power maximization has been previously performed [14,17] without regard for efficiency.

Here, we consider a radiative heat engine performing isentropic energy conversion, similar to the approach considered by Landsberg for solar energy conversion [14,17]. Approaching such an isentropic conversion process in practice requires the radiative heat engine to combine an infinite number of endoreversible subengines connected via nonreciprocal optical components [18,28,29] [see Fig. 1(d)]. Considering an engine temperature T_E and emitted power density $P_E = \sigma T_E^4$, the power output and efficiency are [14]

$$\rho_N = 1 - \frac{4}{3}\frac{T_C}{T_H} - \left(\frac{T_E}{T_H}\right)^4 \left[1 - \frac{4}{3}\frac{T_C}{T_E}\right], \tag{6}$$

$$\eta_N = \frac{\rho_N}{1 - \left(\frac{T_E}{T_H}\right)^4}. \tag{7}$$

Equations (6) and (7) can be applied to calculate the power output and the efficiency for all engine temperatures $0 \leq T_E \leq T_H$, leading to the *nonreciprocal bound* for radiative energy conversion. The power output is maximized for $T_E = T_C$, leading to

$$\bar{\rho}_N = 1 - \frac{4}{3}\frac{T_C}{T_H} + \frac{1}{3}\left(\frac{T_C}{T_H}\right)^4, \tag{8}$$

which gives $\bar{\rho}_N = 93.33\%$ for $T_C = 300$ K and $T_H = 6000$ K, the absolute (Landsberg) limit for solar energy conversion [14,17]. In the limit $T_E \to T_H$, the efficiency tends to the Carnot limit η_C as the power output goes to 0. We note that operating at $T_E \leq T_C$ is always suboptimal as both efficiency and power can increase from that point. By combining Eqs. (6) and (7), we can also write a closed-form expression between η_N and ρ_N, independent of T_E:

$$\eta_N = 1 - \frac{4}{3}\frac{\eta_N}{\rho_N}\frac{T_C}{T_H}\left[1 - \left(1 - \frac{\rho_N}{\eta_N}\right)^{3/4}\right]. \tag{9}$$

We have thus obtained simple analytical expressions for the universal thermodynamic bound of radiative energy conversion between bodies at temperatures T_H and T_C. A blackbody emitter is optimal as it offers the highest incident power and, therefore, the highest power output for any given efficiency.

We compare in Fig. 2 the power-versus-efficiency bounds for the endoreversible model [Eqs. (3) and (4)], the reciprocal bound (see Supplemental Material [27]) and the nonreciprocal bound [Eqs. (6) and (7)], considering an emitter temperature $T_H = 600$ K and a sink temperature $T_C = 300$ K. We note that these bounds are only a function of the temperature *ratio* T_C/T_H, as seen from the closed-form expressions [Eqs. (5) and (9)]. Crucially, the reciprocal bound only marginally surpasses the endoreversible model. Since it can be calculated very simply [Eq. (5)], the endoreversible engine model is, therefore, a useful approximation for the upper bound of reciprocal systems, and we will use both interchangeably in the following.

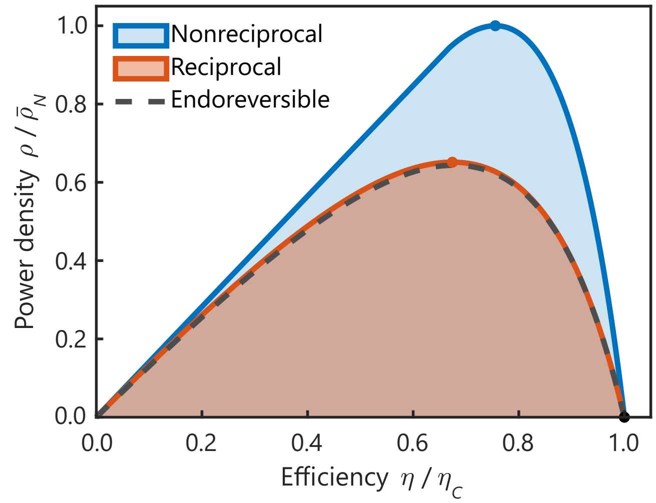

FIG. 2. Thermodynamic performance bounds for radiative energy conversion: maximum power output ρ (normalized to the nonreciprocal limit $\bar{\rho}_N$) as a function of the efficiency η (normalized to the Carnot efficiency η_C) for the nonreciprocal bound (blue area), the reciprocal bound (red area) and the endoreversible engine model (dashed black line). The emitter temperature is $T_H = 600$ K and the sink temperature is $T_C = 300$ K.

Next, we show in Fig. 3 the nonreciprocal and reciprocal bounds for different emitter temperatures. We observe that the relative difference between both bounds tends to be more significant as the emitter temperature decreases or when the efficiency approaches the Carnot limit (see Supplemental Material [27] for a figure with their ratio). Furthermore, we can show that the endoreversible model and the nonreciprocal bound are bounded by

$$\rho_E \leq 4\frac{T_H}{T_C}\eta_E(\eta_C - \eta_E), \tag{10}$$

$$\rho_N \leq 8\frac{T_H}{T_C}\eta_N(\eta_C - \eta_N), \tag{11}$$

and that these bounds are approached as $T_E \to T_H$ (first-order approximation). Therefore, introducing nonreciprocity enables twice as much power output when operating close to the Carnot limit. We also emphasize that Eqs. (10) and (11) follow the quadratic form of the "universal" bounds derived in previous works [24,25].

Last, we focus on the trade-off between power output and efficiency in radiative heat engines by comparing their efficiency at maximum power to that of linear heat engines.

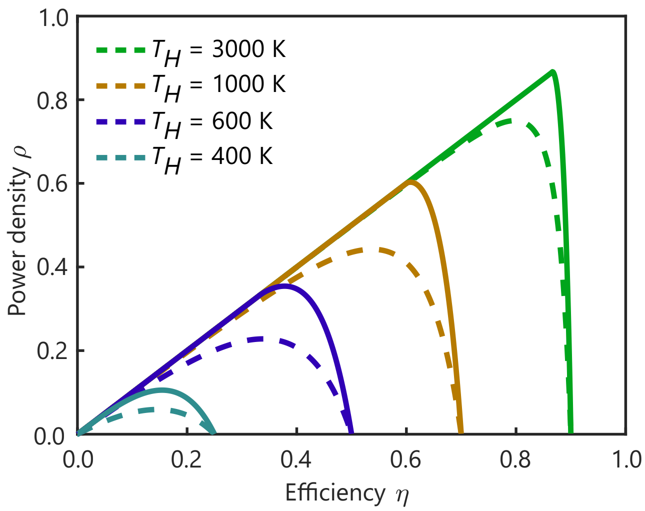

FIG. 3. Nonreciprocal (solid lines) and reciprocal (dashed lines) performance bounds in terms of maximum power output ρ as a function of the efficiency η for different emitter temperatures. The sink temperature is $T_C = 300$ K.

For linear heat engines, the Curzon-Ahlborn limit, originally derived for endoreversible heat engines [19], was shown to extend to all irreversible linear engines [20]. For nonlinear heat engines, efficiency at maximum power has been previously derived, albeit only for endoreversible engines [21]. When T_H tends to T_C, the behavior of radiative heat engines becomes linear, so their efficiency at maximum power approaches the Curzon-Ahlborn limit $\eta_{CA} \approx \eta_C/2$. Beyond the linear approximation, we show the efficiency at maximum power for the endoreversible model and the reciprocal bound in Fig. 4. We observe that the efficiency at maximum power for a given temperature ratio T_H/T_C follows $\bar{\eta_N} \geq \bar{\eta_E} \geq \eta_{CA}$. This result, which originates from nonlinearity [21], highlights that radiative heat engines, such as TPV cells can achieve a better trade-off between power output and efficiency than conventional linear heat engines, particularly for large temperature ratios. Furthermore, for nonlinear engines such as radiative heat engines, nonreciprocity can be exploited to achieve performance beyond endoreversible thermodynamics.

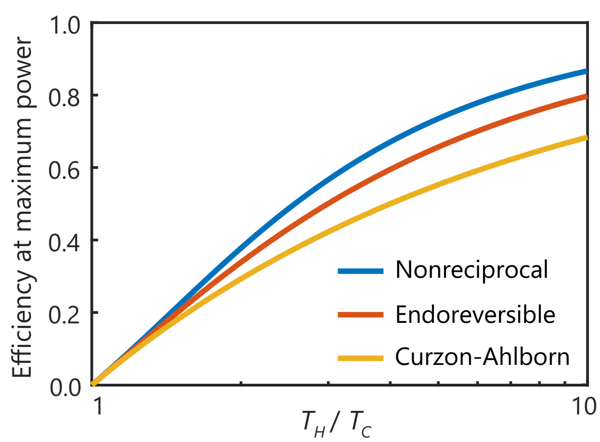

FIG. 4. Efficiency at maximum power for different bounds as a function of the temperature ratio T_H/T_C.

Despite their broad validity, the bounds derived here may be overcome in two cases. The first is near-field operation, where the heat transferred from the emitter to the engine can be much larger than in the far field [30]. The second is the introduction of a heat engine on the hot side, either to increase the power radiated to the cold side (thermophotonics [31]) or to generate additional power output on the hot side (thermoradiative cells [9,10,32]).

In conclusion, we derive thermodynamic performance bounds for radiative energy conversion, expressed in terms of the maximum power achievable for any efficiency. In doing so, we integrate the limits derived over the previous decades for solar energy conversion within a larger thermodynamic framework. The nonreciprocal bound, which has a simple analytical expression, establishes the universal performance limit of radiative heat engines. At the same time, the endoreversible engine model offers a good approximation for the bound of reciprocal engines. We show that nonreciprocal systems may significantly outperform reciprocal ones, especially for low emitter temperatures or when operating at high efficiency. We also reveal that radiative heat engines may achieve a better power-efficiency trade-off than conventional linear engines, especially for high-temperature sources. These results add to the attractive potential of TPV systems for high-temperature energy conversion and offer useful figures of merits and bounds for their comparison.

Acknowledgments. M.G. would like to thank Daniel Suchet for stimulating discussions. This work has been supported in part by the "la Caixa" Foundation (ID 100010434), the Spanish MICINN (PID2021-125441OA-I00, PID2020-112625GB-I00, and CEX2019-000910-S), the European Union (fellowship LCF/BQ/PI21/11830019 under the Marie Skłodowska-Curie Grant Agreement No. 847648), Generalitat de Catalunya (2021 SGR 01443), Fundació Cellex, and Fundació Mir-Puig. M.G. and M.F.P. acknowledge financial support from the Severo Ochoa Excellence Fellowship.

[1] N. M. Haegel *et al.*, Photovoltaics at multi-terawatt scale: Waiting is not an option, Science **380**, 39 (2023).
[2] A. Datas and R. Vaillon, in *Ultra-High Temperature Thermal Energy Storage, Transfer and Conversion*, Woodhead Publishing Series in Energy, edited by A. Datas (Woodhead Publishing, 2021), p. 285.
[3] B. Lee, R. Lentz, T. Burger, B. Roy-Layinde, J. Lim, R. M. Zhu, D. Fan, A. Lenert, and S. R. Forrest, Air-bridge Si thermophotovoltaic cell with high photon utilization, ACS Energy Lett. **7**, 2388 (2022).

[4] A. LaPotin, K. L. Schulte, M. A. Steiner, K. Buznitsky, C. C. Kelsall, D. J. Friedman, E. J. Tervo, R. M. France, M. R. Young, A. Rohskopf, S. Verma, E. N. Wang, and A. Henry, Thermophotovoltaic efficiency of 40%, Nature **604**, 287 (2022).

[5] E. López, I. Artacho, and A. Datas, Thermophotovoltaic conversion efficiency measurement at high view factors, Solar Energy Mater. Sol. Cells **250**, 112069 (2023).

[6] A. Datas, A. López-Ceballos, E. López, A. Ramos, and C. del Cañizo, Latent heat thermophotovoltaic batteries, Joule **6**, 418 (2022).

[7] W. Greiner, L. Neise, and H. Stöcker, *Thermodynamics and Statistical Mechanics*, Classical theoretical physics (Springer-Verlag, New York, 1995).

[8] G. Benenti, K. Saito, and G. Casati, Thermodynamic bounds on efficiency for systems with broken time-reversal symmetry, Phys. Rev. Lett. **106**, 230602 (2011).

[9] S. Buddhiraju, P. Santhanam, and S. Fan, Thermodynamic limits of energy harvesting from outgoing thermal radiation, Proc. Natl. Acad. Sci. **115**, E3609 (2018).

[10] Y. Park, Z. Omair, and S. Fan, Nonreciprocal thermophotovoltaic systems, ACS Photonics **9**, 3943 (2022).

[11] W. Shockley and H. J. Queisser, Detailed balance limit of efficiency of p-n junction solar cells, J. Appl. Phys. **32**, 510 (1961).

[12] R. T. Ross and A. J. Nozik, Efficiency of hot-carrier solar energy converters, J. Appl. Phys. **53**, 3813 (1982).

[13] M. Giteau, S. Almosni, and J.-F. Guillemoles, Hot-carrier multi-junction solar cells: A synergistic approach, Appl. Phys. Lett. **120**, 213901 (2022).

[14] M. A. Green, *Third Generation Photovoltaics Advanced Solar Energy Conversion* (Springer, Berlin; Heidelberg, 2003).

[15] A. D. Vos, Reflections on the power delivered by endoreversible engines, J. Phys. D: Appl. Phys. **20**, 232 (1987).

[16] A. De Vos, The endoreversible theory of solar energy conversion: A tutorial, Solar Energy Mater. Sol. Cells **31**, 75 (1993).

[17] P. T. Landsberg and G. Tonge, Thermodynamic energy conversion efficiencies, J. Appl. Phys. **51**, R1 (1980).

[18] H. Ries, Complete and reversible absorption of radiation, Appl. Phys. B **32**, 153 (1983).

[19] F. L. Curzon and B. Ahlborn, Efficiency of a Carnot engine at maximum power output, Am. J. Phys. **43**, 22 (1975).

[20] C. Van den Broeck, Thermodynamic efficiency at maximum power, Phys. Rev. Lett. **95**, 190602 (2005).

[21] A. De Vos, Efficiency of some heat engines at maximum-power conditions, Am. J. Phys. **53**, 570 (1985).

[22] S. Göktun, S. Özkaynak, and H. Yavuz, Design parameters of a radiative heat engine, Energy **18**, 651 (1993).

[23] A. Datas, Optimum semiconductor bandgaps in single junction and multijunction thermophotovoltaic converters, Solar Energy Mater. Sol. Cells **134**, 275 (2015).

[24] N. Shiraishi, K. Saito, and H. Tasaki, Universal trade-off relation between power and efficiency for heat engines, Phys. Rev. Lett. **117**, 190601 (2016).

[25] P. Pietzonka and U. Seifert, Universal trade-off between power, efficiency, and constancy in steady-state heat engines, Phys. Rev. Lett. **120**, 190602 (2018).

[26] T. Burger, C. Sempere, B. Roy-Layinde, and A. Lenert, Present efficiencies and future opportunities in thermophotovoltaics, Joule **4**, 1660 (2020).

[27] See Supplemental Material at http://link.aps.org/supplemental/10.1103/PhysRevApplied.20.L061003 for a general derivation of the reciprocal bound and a figure presenting the ratio between the powers obtained with the reciprocal and nonreciprocal bounds.

[28] M. A. Green, Time-asymmetric photovoltaics, Nano Lett. **12**, 5985 (2012).

[29] Y. Park, B. Zhao, and S. Fan, Reaching the ultimate efficiency of solar energy harvesting with a nonreciprocal multijunction solar cell, Nano Lett. **22**, 448 (2022).

[30] M. Laroche, R. Carminati, and J.-J. Greffet, Near-field thermophotovoltaic energy conversion, J. Appl. Phys. **100**, 063704 (2006).

[31] N.-P. Harder and M. A. Green, Thermophotonics, Semicond. Sci. Technol. **18**, S270 (2003).

[32] R. Strandberg, Theoretical efficiency limits for thermoradiative energy conversion, J. Appl. Phys. **117**, 055105 (2015).